

Comparison and Repeatability of High Resolution and High Speed Scans from Spectralis Optical Coherence Tomography Angiography

Federico Corvi¹⁻³, Giulia Corradetti^{1,2}, Salvatore Parrulli³, Lucia Pace³, Giovanni Staurenghi³, and Srinivas R. Sadda^{1,2}

¹ Doheny Image Reading Center, Doheny Eye Institute, Los Angeles, CA, USA

² Department of Ophthalmology, David Geffen School of Medicine at UCLA, Los Angeles, CA, USA

³ Eye Clinic, Department of Biomedical and Clinical Science "Luigi Sacco," Sacco Hospital, University of Milan, Milan, Italy

Correspondence: Srinivas R. Sadda, Doheny Eye Institute, Department of Ophthalmology, David Geffen School of Medicine at UCLA, 1355 San Pablo Street, Los Angeles, CA, 90033, USA. e-mail: ssadda@doheny.org

Received: June 29, 2020

Accepted: August 24, 2020

Published: September 28, 2020

Keywords: optical coherence tomography angiography (OCTA); repeatability; vessel density; vessel length density; choriocapillaris

Citation: Corvi F, Corradetti G, Parrulli S, Pace L, Staurenghi G, Sadda SR. Comparison and repeatability of high resolution and high speed scans from spectralis optical coherence tomography angiography. *Trans Vis Sci Tech.* 2020;9(10):29. <https://doi.org/10.1167/tvst.9.10.29>

Purpose: The purpose of this study was to evaluate and compare the repeatability of optical coherence tomography angiography (OCTA) derived retinal vascular quantitative metrics using high resolution (HR) versus high speed (HS) acquisition modes.

Methods: Macular 4.4 × 2.9-mm OCTA images from normal, healthy volunteers were captured using both HR (768 A-scans × 256 B-scans) and HS (384 A-scans × 256 B-scans) acquisition protocols. Vessel density and vessel length density of the superficial capillary plexus and deep capillary plexus, as well as choriocapillaris flow deficit were computed. In a subset of eyes, the OCTA scans were repeated twice 2 days later and the same metrics were recomputed to assess repeatability, using intraclass correlation coefficients and coefficient of variation (CV).

Results: Comparison of measurements between HR and HS acquisitions in 41 healthy eyes showed statistically significant differences for all quantitative metrics ($P < 0.01$). However, no significant differences were observed among the three repeated scans (one on day 1 and two on day 3) obtained with each of the acquisition modes. The CVs ranged from 0.01 to 0.03 with the HR mode and 0.01 to 0.04 with the HS mode. The intraclass correlation coefficients (ICCs) among measurements were similar and high for both HR and HS modes, ranging from 0.844 to 0.949.

Conclusions: HR and HS OCTA acquisition modes both yielded repeatable quantitative metrics for the retinal circulation and the choriocapillaris. However, despite a similar field, the HR and HS derived measurements differed significantly.

Translational Relevance: To establish OCTA imaging in clinical and research practice, standardized and repeatability image analysis are necessary.

Introduction

Optical coherence tomography angiography (OCTA) represents a significant advance in retinal imaging, which allows the retinal microvasculature of the retina to be imaged and quantified in a rapid and noninvasive fashion.^{1,2} In contrast to standard dye imaging techniques, such as fluorescein angiography and indocyanine green angiography, OCTA is sufficiently depth-resolved to allow the various retinal vascular layers to be visualized.² In addition, OCTA

images are of very high contrast and not impacted by diffusion of dye, which also aids in superior visualization of the vasculature. On the other hand, OCTA imaging may be susceptible to various pitfalls and artifacts, including motion artifacts, segmentation errors, and projection artifacts.³

Another significant capability of OCTA is the ability to quantitatively evaluate the superficial and deep retinal capillary plexuses and the choriocapillaris. A number of studies have evaluated these quantitative OCTA biomarkers in various diseases.^{2,4-6} Incorporation of these quantitative parameters into clinical trials

Table 1. High Resolution and High-Speed Acquisition Parameters

	High Resolution	High Speed
Scan angle	15 degrees	15 degrees
Pattern size	15 degrees × 10 degrees 4.4 × 2.9 mm	15 degrees × 10 degrees 4.4 × 2.9 mm
Size X	768 pixels 4.4 mm	384 pixels 4.4 mm
Size Z	496 pixels 1.9 mm	496 pixels 1.9 mm
Scaling X (approximate)	5.73 μm/pixels	11.46 μm/pixels
Scaling Z (approximate)	3.87 μm/pixels	3.87 μm/pixels
Automatic real-time tracking	5 images	5 images
Number of B-scans	256	256
Distance between B-scans	12 μm	12 μm

and clinical practice requires that their repeatability and reproducibility be established. A number of studies have evaluated the reliability of these metrics among various OCTA instruments. It has been found that measurements from the various OCTA instruments are not interchangeable and this has been attributed to various factors that may differ between devices, such as laser light source wavelength, scan dimensions, and OCTA processing algorithm.^{7–12} The Spectralis OCTA device utilized a probabilistic algorithm to identify motion (i.e. flow) between a series of repeated scans. The Spectralis OCTA also allows many attributes of the OCTA acquisition to be customized, including the number of A-scans, B-scans, and spacing between scans. This allows the user to select between scan acquisition modes emphasizing resolution (i.e. more A-scans) at the expense of speed, or speed (i.e. shorter acquisition time) at the expense of resolution. Which mode is preferred may be determined based on the specific clinical needs. However, before these different modes can be used confidently, it would be important to establish their repeatability and whether they could be used interchangeably.

For this reason, in this study, we compare OCTA quantitative metrics from the retinal circulation and choriocapillaris in healthy subjects using both the high speed (HS) and high resolution (HR) acquisition modes.

Methods

Participants

This was a multicenter, cross-sectional prospective study with subjects recruited from the Doheny-University of California Los Angeles (UCLA) Eye Centers and the Eye Clinic of Luigi Sacco

Hospital. The study was performed in accordance with the Health Insurance Portability and Accountability Act and adhered to the principles of the Declaration of Helsinki. Institutional review board (IRB) approval was obtained from the UCLA IRB (Los Angeles, CA) and from the Luigi Sacco Hospital (Ethical committee Milan Area 3).

Consecutive healthy volunteers with no systemic or ocular disease, as confirmed by history and ophthalmic examination, were recruited between May 1 and May 31, 2020. Written, informed consent was obtained from all subjects prior to image acquisition. All participants underwent complete ophthalmic examination, ocular biometry, and OCTA.

Image Acquisition

Patients were imaged using the Spectralis OCTA version 6.12.3.0 (Spectralis, Heidelberg Engineering, Heidelberg, Germany) with two different scan acquisition protocols (Table 1), both with a 15 degree field of view, 4.4 × 2.9-mm X by Y dimension on the retina, 256 B-scans (12 μm between B-scans), a Z-dimension of 1.9 mm (496 pixels approximated to 3.87 μm/pixel), and automatic real-time tracking (ART) of 5.

For the HR protocol, the X-dimension consisted of 768 pixels over the 4.4 mm (approximated to 5.73 μm/pixel), whereas for the HS protocol the X-dimension consisted of 384 pixels over the 4.4 mm (approximated to 11.46 μm/pixel).

To assess repeatability, a subset of this cohort agreed to return 2 days later (day 3) and these same acquisitions (HR and HS) were repeated twice using the same device and same operator on the same eye (Fig. 1).

The operator was specifically trained to the study protocol and was required to check for good focus, absence of motion artifact (identified by horizontal misalignment of vessel segments on en face images),

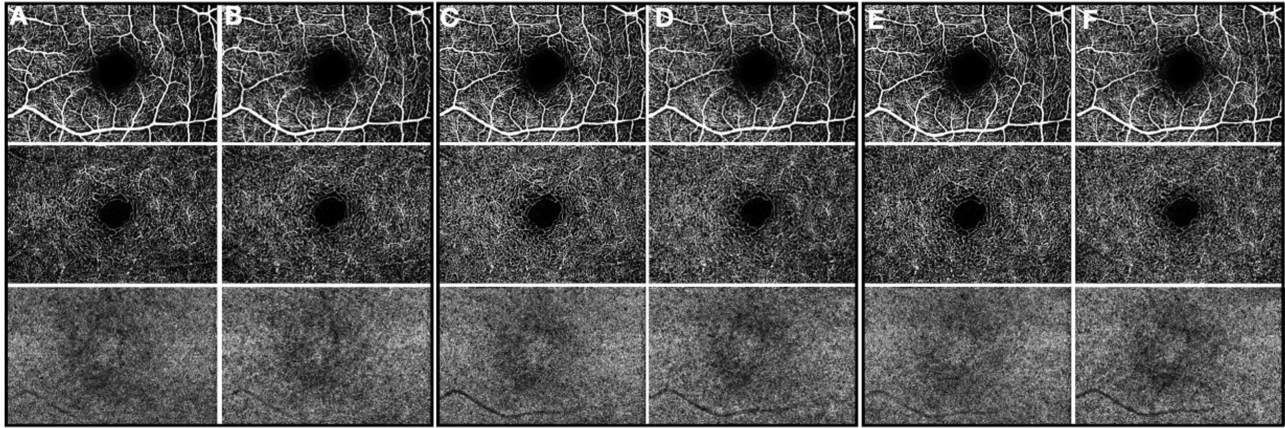


Figure 1. OCT Angiography of an eye imaged on day 1 (A, B), day 3 first scan (C, D) and day 3 third scan (E, F). En face optical coherence tomography angiography (OCTA) of the superficial capillary plexus (first row), deep capillary plexus (second row), and choriocapillaris (third row) obtained with high resolution A, C, and E and high speed B, D, F using the Spectralis OCTA.

good centration, and the use of the follow-up function to ensure the same area of examination. For an eye to be included in the final analysis, a signal-to-noise ratio > 30 decibels had to be achieved across all of the scan acquisitions.

For each scan acquisition for each patient, the time measured in seconds with a chronograph was recorded.

OCTA Analysis

The manufacturer's fully automated retinal layer segmentation algorithm was applied to the 3-dimensional OCTA volumes in order to segment the superficial capillary plexus (SCP), deep capillary plexus (DCP), and choriocapillaris (CC). The CC was segmented using a 20- μm slab, offset 21 μm deep to the retinal pigment epithelium (RPE) band centerline. The manufacturer's projection removal software was used to remove residual artifacts from the overlying retinal circulation for quantification of the DCP and CC.

After confirming proper segmentation, en face images from the SCP, DCP, and CC were exported from the instrument and then imported into the freely available FIJI software (an expanded version of ImageJ version 1.51a; fiji.sc) for computation of vessel metrics (Fig. 2). Vessel density (VD) was defined as the total area of vasculature per unit area in a region of measurement. VD for SCP was computed in accordance with prior reports.^{13,14} In brief, images were duplicated in order to apply two binarization methods. One image was processed first by a Hessian filter, followed by global thresholding using Huang's fuzzy thresholding method. The other duplicate image was binarized using median local thresholding. Finally,

the two different binarized images were combined to generate the final binarized image in which only pixels that existed on both binarized images were included. VD was then assessed on this final resultant image.

To calculate the VD for DCP, the manufacturer's projection removal software was first applied, and then to remove the impact of any residual projections, the superficial large retinal vessels were excluded from quantitative analysis, as previously described.^{13,14} VD was then assessed on this final resultant image.

Vessel length density (VLD) was defined as the vessel length per unit area and was computed after skeletonization of the image, as previously described.¹⁴⁻¹⁶

For CC analysis, CC flow deficits (FDs) were measured using the Phansalkar method (radius = 21.5 μm), as described previously.^{17,18} Small flow deficits (diameter less than approximately 24 μm) were removed from the obtained map, as they are believed to be within the range of normal intercapillary spacing and within normal oxygen diffusion capability.¹⁹ The CC directly beneath major superficial retinal vessels was excluded from the analysis to eliminate potentially confounding residual shadow or projection artifacts, as previously described.¹³ The FD was counted as the percentage of the area analyzed using the "Analyze Particles" command. The CC analysis was performed for the entire slab, as well as for the nasal and temporal halves to confirm consistency of the results.

To confirm the grading repeatability of the analysis method, the entire process and measurements were repeated twice by two certified, independent Doheny Image Reading Center OCTA graders (F.C. and G.C.).

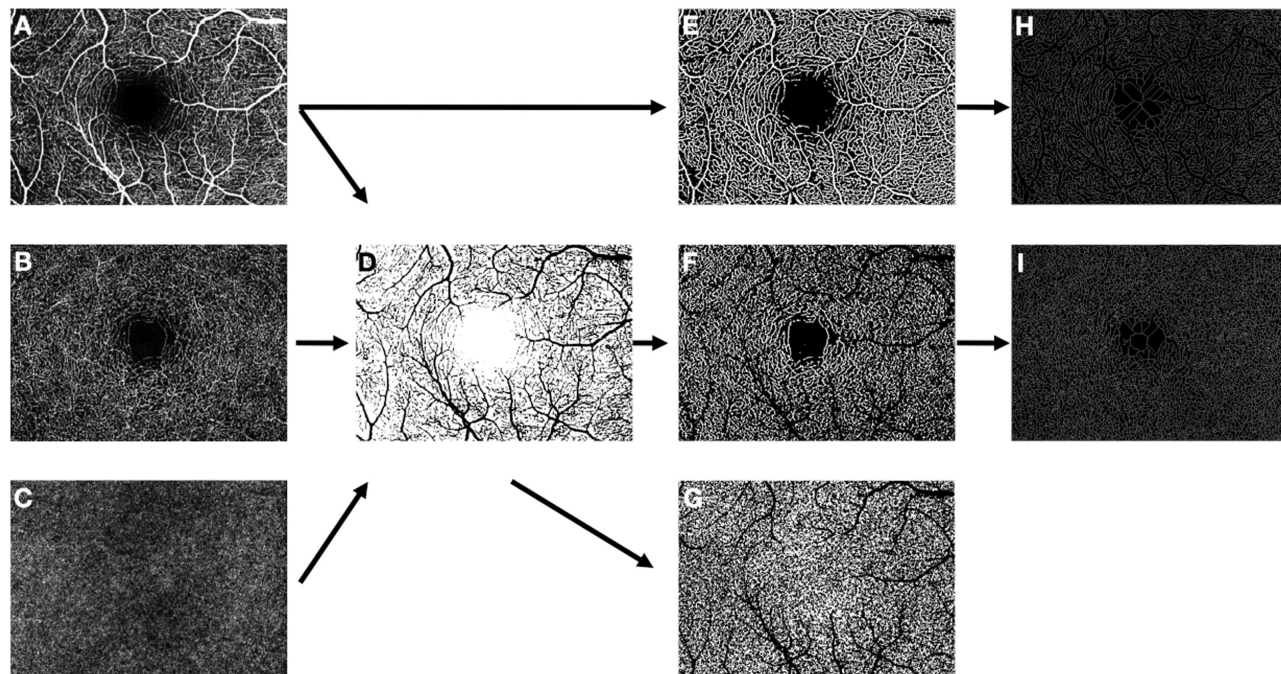


Figure 2. Computation of retinal vessel density (VD), retinal vessel length density (VLD), and choriocapillaris flow deficit (FD) using optical coherence tomography angiography (OCTA). En face slabs of the superficial capillary plexus (A), deep capillary plexus (B), and choriocapillaris (C) were exported. The superficial capillary plexus slab was used to create a mask (D) to exclude these regions and eliminate potentially confounding shadow artifacts in the DCP and CC images. Binarized images (E, F, G) were used to compute superficial E and deep F capillary plexus VD and choriocapillaris FD G, and skeletonized images (H, I) were used to compute the VLD of the superficial H and deep capillary plexus I.

Statistical Analysis

Statistical analyses were performed using SPSS version 26.0 (IBM Corporation, Armonk, NY). Tests for normality of data were first conducted using the Kolmogorov–Smirnov and Shapiro–Wilk analysis. HR and HS acquisition protocols were compared using VD and VLD of SCP and DCP, and CC FD from the first acquisition (“Baseline visit”) using the Student’s *t*-test for paired samples and Wilcoxon signed-rank test according to data distribution. For the subset of subjects that agreed to return for two additional acquisitions at the second visit (day 3), all three acquisitions (one at baseline and two on day 3), repeated measures analysis of variance (ANOVA) and the Friedman test were performed according to sample distribution to evaluate mean differences in the high resolution series and high speed series over the three measurements. The repeatability of the measurements was assessed using both intraclass correlation coefficient (ICC) and coefficient of variation (CV). The CV is the ratio of the standard deviation (SD) and the mean and a value closer to 0 reflects higher repeatability. Bland-Altman plots were also constructed to assess the limits of agreement for the various quantitative retinal metrics

between HR and HS acquisition modes. The ICCs were calculated to measure the intergrader repeatability for quantitative assessments. A *P* value < 0.05 was considered to be statistically significant.

Results

Of the 53 consecutive healthy volunteers imaged with the Spectralis OCTA with both HS and HS protocols, 12 had to be excluded from the analysis because they did not meet all of the prespecified criteria for quality for all scans (HR and HS). One eye per subject was included in the analysis for a total of 41 eyes. Nineteen (46.3%) were women and 22 (54%) were men with a mean age of 36.19 years (SD, 12.21; range, 25–69 years). The mean axial length was 24.32 mm (SD = 1.15 mm; range = 22.11–26.88).

The mean values of VD and VLD for SCP and DCP and the mean values of CC FD for the HR and HS acquisitions are shown in Table 2 and Figure 3, and demonstrated significant differences. For example, the mean VD of the SCP and DCP was greater for the HS protocol than HR ($P < 0.0001$). On the other side,

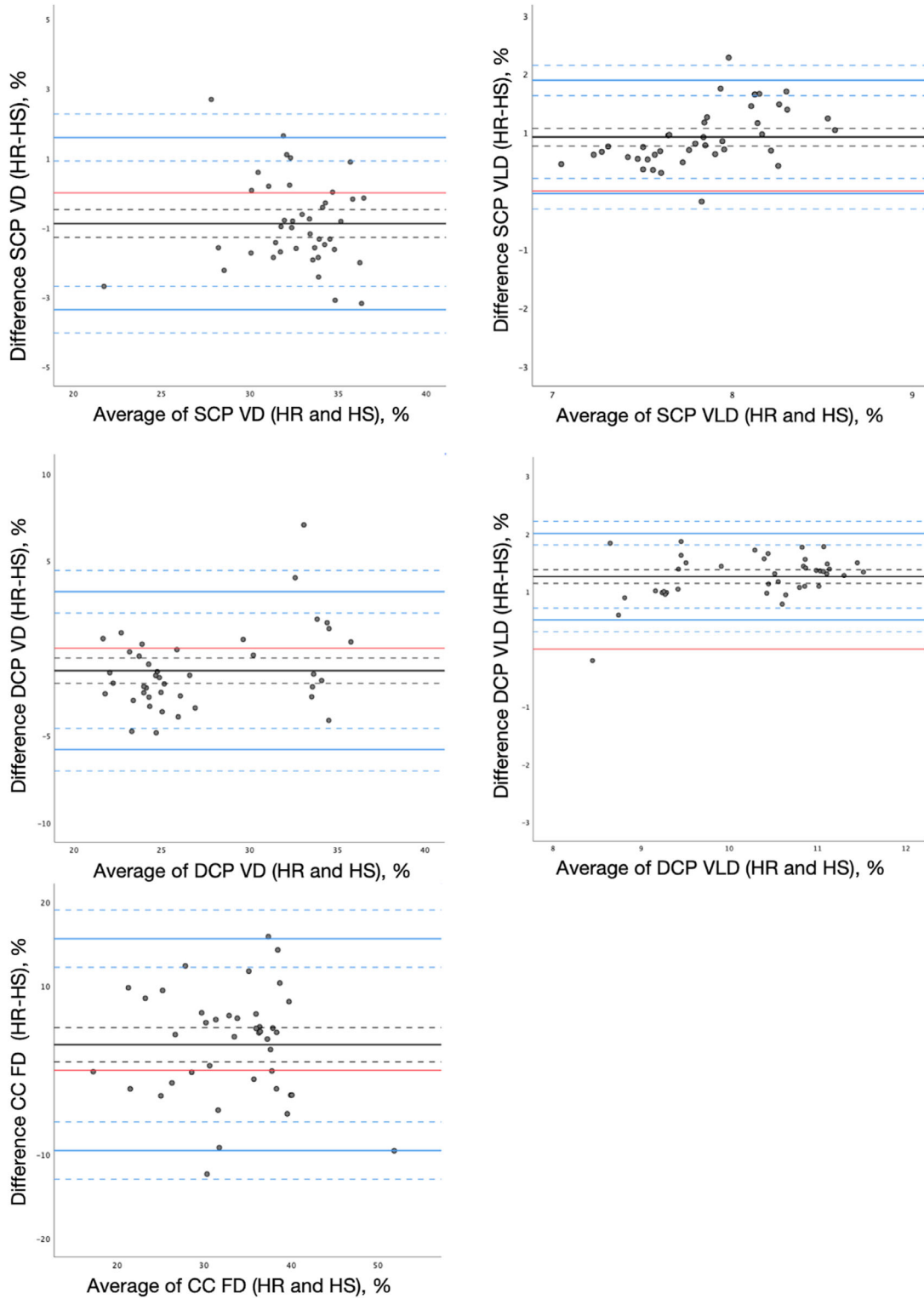


Figure 3. Bland-Altman plots comparing the various quantitative retinal vessel metrics between high resolution and high-speed modes. The *black lines* indicate the mean difference between high resolution and high speed, whereas the *black dashed lines* denote the 95% confidence intervals. The *blue lines* show the upper and lower limits of agreements, whereas the *blue dashed lines* denote the corresponding 95% confidence intervals. The red line denotes the zero difference between high resolution and high-speed modes.

Table 2. Comparison of Vessel Metrics With High Resolution and High-Speed Acquisition Protocols

	High Resolution	High Speed	<i>P</i> Value
SCP VD	32.18 ± 2.80	33.07 ± 2.86	<0.0001
SCP VLD	8.30 ± 0.53	7.38 ± 0.30	<0.0001
DCP VD	26.47 ± 5.09	27.75 ± 4.25	<0.0001
DCP VLD	10.88 ± 0.97	9.62 ± 0.82	<0.0001
CC FD entire slab	34.77 ± 7.06	31.72 ± 7.57	0.004
CC FD nasal	34.51 ± 6.88	31.61 ± 8.04	0.008
CC FD temporal	35.04 ± 7.71	31.84 ± 7.88	0.004

Student's *t*-test for paired samples and Wilcoxon signed-rank test were performed to compare high resolution and high-speed modes. CC, choriocapillaris; CI, confidence interval; DCP, deep capillary plexus; FD, flow deficit; SCP, superficial capillary plexus; VD, vessel density; VLD, vessel length density.

Table 3. Vessel Metrics Over Time

High resolution	Baseline	Day 3–Scan 1	Day 3–Scan 2	<i>P</i> Value
SCP VD	33.23 ± 1.41	33.26 ± 1.39	33.15 ± 2.14	0.979
SCP VLD	8.22 ± 0.55	8.27 ± 0.44	8.24 ± 0.49	0.940
DCP VD	23.21 ± 1.39	23.31 ± 1.57	25.04 ± 1.98	0.874
DCP VLD	11.49 ± 0.37	11.65 ± 0.42	11.55 ± 0.56	0.524
CC FD	36.43 ± 5.11	36.22 ± 6.57	36.03 ± 6.86	0.978
Time	33.21 ± 5.43	33.25 ± 6.18	33.43 ± 5.91	0.925
High Speed	Baseline	Day 3–Scan 1	Day 3–Scan 2	<i>P</i> Value
SCP VD	33.86 ± 1.88	33.63 ± 1.92	33.97 ± 1.87	0.854
SCP VLD	7.33 ± 0.31	7.45 ± 0.30	7.42 ± 0.24	0.402
DCP VD	25.09 ± 1.73	23.08 ± 1.49	25.61 ± 1.67	0.491
DCP VLD	10.14 ± 0.39	10.24 ± 0.41	10.24 ± 0.38	0.595
CC FD	30.37 ± 5.86	30.86 ± 7.34	30.33 ± 7.45	0.964
Time	22.04 ± 5.3	21.96 ± 5.25	22.42 ± 5.4	0.951

Repeated measurements were evaluated with the Friedman test and the repeated measures analysis of variance (ANOVA). CC, choriocapillaris; DCP, deep capillary plexus; FD, flow deficit; SCP, superficial capillary plexus; VD, vessel density; VLD, vessel length density.

the mean VLD of the SCP and DCP was greater for the HR protocol than HS ($P < 0.0001$). The CC FDs for the entire slab, as well as the nasal and temporal sections, were greater for the HR protocol than the HS ($P = 0.004$, $P = 0.008$, and $P = 0.004$, respectively). The CC FD of the nasal section was not significantly different than the temporal section for the HR (34.51 ± 6.88 and 35.04 ± 7.71 , $P = 0.372$) protocol and for the HS protocol (31.61 ± 8.04 and 31.84 ± 7.88 , $P = 0.772$).

Of the 53 subjects originally recruited for the study, 28 returned and were successfully imaged with the same scan patterns twice 2 days later (day 3). Four were excluded from the analysis because of poor scan quality and, thus, 24 eyes were included in the repeatability analysis. The mean values of VD and VLD for SCP and DCP, CC FD, and scan time for both HR and HS

scans for the three acquisitions are shown in [Table 3](#). No significant differences were observed for any of the parameters over the three scans.

Repeatability was assessed with ICC and CV, as shown in [Table 4](#). The CVs ranged from 0.01 to 0.05 for the HR scans and 0.01 to 0.07 for the HS scans, and the ICCs were similar and high for both HR and HS scans.

The ICC between graders to assess the vascular quantitative metrics was also high in the HR mode with values of 0.928 for VD in the SCP (95% confidence interval [CI] = 0.888–0.953), 0.987 for VD in the DCP (95% CI = 0.980–0.991), 0.888 for VLD in the SCP (95% CI = 0.829–0.926), 0.926 for VLD in the DCP (95% CI = 0.886–0.951), and 0.991 for CC FD (95% CI = 0.987–0.994). Similarly, the ICC was also high for the HS mode with values of 0.93 for VD in the SCP (95%

Table 4. Repeatability of High Resolution and High-Speed Scans

	Day 1	Day 3–Scan 1	Day 3–Scan 2	ICC	CV
SCP VD	33.23 ± 1.41	33.26 ± 1.39	33.15 ± 2.14	0.856 (0.714–0.933)	0.01
High resolution				<i>P</i> < 0.0001	
SCP VD	33.86 ± 1.88	33.63 ± 1.92	33.97 ± 1.87	0.844 (0.693–0.927)	0.02
High speed				<i>P</i> < 0.0001	
SCP VLD	8.22 ± 0.55	8.27 ± 0.44	8.24 ± 0.49	0.949 (0.9–0.976)	0.02
High resolution				<i>P</i> < 0.0001	
SCP VLD	7.33 ± 0.31	7.45 ± 0.30	7.42 ± 0.24	0.933 (0.857–0.97)	0.02
High speed				<i>P</i> < 0.0001	
DCP VD	23.21 ± 1.39	23.31 ± 1.57	25.04 ± 1.98	0.850 (0.704–0.930)	0.01
High resolution				<i>P</i> < 0.0001	
DCP VD	25.09 ± 1.73	23.08 ± 1.49	25.61 ± 1.67	0.883 (0.77–0.946)	0.01
High speed				<i>P</i> < 0.0001	
DCP VLD	11.49 ± 0.37	11.65 ± 0.42	11.55 ± 0.56	0.868 (0.742–0.938)	0.02
High resolution				<i>P</i> < 0.0001	
DCP VLD	10.14 ± 0.39	10.24 ± 0.41	10.24 ± 0.38	0.885 (0.776–0.946)	0.02
High speed				<i>P</i> < 0.0001	
CC FD	36.43 ± 5.11	36.22 ± 6.57	36.03 ± 6.86	0.944 (0.899–0.974)	0.03
High resolution				<i>P</i> < 0.0001	
CC FD	30.37 ± 5.86	30.86 ± 7.34	30.33 ± 7.45	0.935 (0.871–0.97)	0.04
High speed				<i>P</i> < 0.0001	
Time	33.21 ± 5.43	33.25 ± 6.18	33.43 ± 5.91	0.965 (0.931–0.984)	0.05
High resolution					
Time	22.04 ± 5.3	21.96 ± 5.25	22.42 ± 5.4	0.959 (0.919–0.981)	0.07
High speed					

CC, choriocapillaris; CV, coefficient of variation; DCP, deep capillary plexus; FD, flow deficit; ICC, intraclass correlation coefficient; SCP, superficial capillary plexus; VD, vessel density; VLD, vessel length density.

CI = 0.894–0.954), 0.983 for VD in the DCP (95% CI = 0.972–0.99), 0.935 for VLD in the SCP (95% CI = 0.910–0.957), 0.879 for VLD in the DCP (95% CI = 0.816–0.92), and 0.921 for CC FD (95% CI = 0.879–0.948).

Discussion

In this study, we observed significant differences in vessel metrics with two different acquisition protocols of the same size on the same OCTA device. The protocols differed only with regard to the resolution of the B-scan with twice as many pixels of acquisition with the HR mode. Despite differences in values between the two modes, the repeatability within each mode was high.

Given the significant interest in using OCTA-derived quantitative metrics in clinical trials and clinical practice, assessing the repeatability of these measurements and identifying the optimal protocol for specific applications is of critical importance.^{2,4}

A number of studies have evaluated the reproducibility and repeatability of different OCTA devices and specific acquisition protocols. Lei et al.²⁰ tested the repeatability and reproducibility of automated OCTA measurements (VLD and VD) of the SCP using three repeated scans with three instruments (Cirrus HD-OCT 5000 with AngioPlex software) finding high levels of repeatability and reproducibility. At the same time, Lee et al.²¹ found relatively good repeatability of VD, VLD, and foveal avascular zone using the HD-OCT 5000 with AngioPlex software in patients with various retinal diseases imaged with two consecutive scans. Al-Sheikh et al.²² tested the repeatability of OCTA-derived automated VD measurements in the SCP and DCP in healthy individuals using the NIDEK RS-3000 Advance device showing high repeatability. Ho et al.²³ compared the 3 × 3-mm and 6 × 6-mm scan protocols using the same device finding better vascular resolution in 3 × 3-mm scan and more clinical information in the 6 × 6-mm scan because of the larger scan area.

In contrast, in our study, we specifically assessed the repeatability of several commonly used

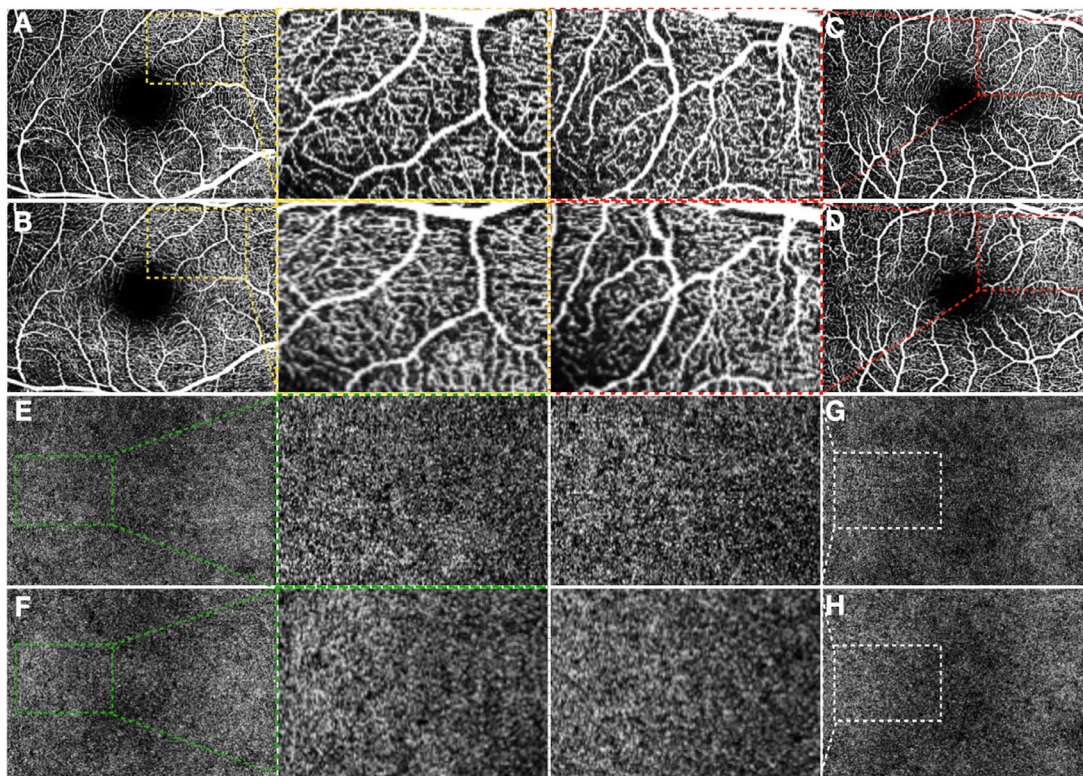


Figure 4. Images of the superficial capillary plexus (**A–D**) and choriocapillaris (**E–H**) imaged with the high resolution **A, C, E, and G** and high speed **B, D, F, and H** modes. The two images seem qualitatively similar at low magnification. However, *four rectangles with yellow, red, green, and white dashed edges* display at high magnification corresponding regions from the high resolution and high-speed images. At this magnification, qualitative differences between HR and HS scans are more readily apparent. Both larger vessels and the smallest capillaries are more distinct with less blurring on the HR images compared to the HS images. Similarly, the choriocapillaris appears more distinct on the HR images compared to the HS images.

quantitative metrics with the Spectralis OCTA device and we extended the analysis to the CC using two different resolutions. Regardless of the resolution used, the repeatability was high in this cohort of healthy subjects with CV values between 0.01 and 0.04 for all evaluated quantitative parameters, and no difference in the level of repeatability between HR and HS modes.

We also evaluated the consistency in the quantitative metrics using the two different acquisition modes. Several previous papers have evaluated the agreement of OCTA devices under different conditions.^{7–9,11,12,20} Magrath et al.⁷ evaluated the variability in foveal avascular zone and VD measurements using RTVue XR Avanti OCTA and AngioPlex OCTA and observed a high level of variability. Corvi et al.⁸ compared seven different OCTA instruments and showed that the VD, FD, and FAZ values for both the SCP and DCP could not be used interchangeably among different OCT devices in healthy subjects. Differences between OCTA devices were also reported for assessing macular neovascularization (MNV) using area, VD, and fractal

dimension of the lesion as well as for assessing diabetic retinopathy based on visualization of microaneurysms in the SCP and DCP.^{10,12} Although OCTA measurements clearly differed among devices from different manufacturers, Lei et al.²⁰ observed that three different OCTA devices of the same model and manufacturer provided reproducible results.

In our study, we also used the same device and even the same field of view, but varied the resolution in one dimension. This change in resolution was sufficient to cause significant differences in measurements. Venogopal JP and colleagues utilized two different scan resolutions (400 vs. 304 A-scans) to evaluate the peripapillary vessel density in normal and glaucomatous eyes using the Optovue RTVue-XR device.²⁴ To the best of our knowledge, however, ours is the first study evaluating the impact of resolution in isolation on OCTA derived vessel metrics from both the superficial and deep retinal capillary plexus of the macula, as well as the CC (Fig. 4). Notably, we observed a higher CC FD for the HR protocol regardless of macular location (nasal versus temporal). The

importance of high resolution to evaluate the CC was also emphasized by Kurokawa et al. who used a research adaptive optics OCTA (AO-OCTA) to evaluate the CC.²⁵ The authors noted that AO-OCTA provided a more complete description of CC capillary morphometry and more consistent results with histology than conventional OCTA due to the better resolution and ability to delineate individual capillaries. Thus, it is not surprising that we observed a higher CC FD with the HR protocol, as higher resolution should mean more clearly defined and less blurry (and thus thinner) capillary segments. Thinner capillaries would mean greater spacing between capillaries and thus consequently a greater CC FD with the HR protocol.

Our findings are of clinical importance as there are significant trade-offs between speed and resolution, which may need to be assessed when selecting the optimal acquisition mode for a particular application. Freund and colleagues have shown that very HR, albeit by increasing the number of B-scans rather than A-scans, can be of benefit in more precisely assessing the relationship between blood flow and fine retinal microstructural abnormalities, such as type 3 MNV.²⁶ On the other hand, higher resolution and greater number of pixels for acquisition will mean longer scan times. In the present study, we observed a 33.7% longer acquisition time for the HR mode compared to the HS mode. Although longer acquisition time may be acceptable in healthy subjects and in research protocols, they may not be practical for routine use in clinical practice, particularly with poor-fixating patients with reduced vision. For such patients, an HS mode may be preferred. It is reassuring to observe that despite a faster acquisition with reduced resolution, the HS mode still provides highly repeatable results.

Our study has several limitations that must be considered when assessing our results. First, we did not evaluate patients with retinal disease, as we tested the repeatability only in healthy volunteers. The presence of retinal disease may impact the stability of fixation, which could influence both repeatability and acquisition time. Second, the sample size was relatively small, particularly for the repeatability analysis. As a result, the study was underpowered to detect very small differences in the various metrics, however, such small differences are less likely to be clinically relevant. Last, we must acknowledge that resolution and B-scan acquisition speed are two independent factors that may both affect the quantitative OCTA metrics. In this study, we compared only the high resolution versus the high speed modes, as provided by the manufacturer. Future studies could consider various combinations of speed (high versus low) and resolution (high

versus low) to more precisely assess the impact of speed and resolution on retinal and choroidal quantitative metrics. On the other hand, a strength of our study is that we not only considered repeatability based on data from within a given day, but over several days, which may provide greater confidence in the repeatability analysis.

In summary, we observed that both HR and HS acquisition modes for the Spectralis OCTA could yield repeatable retinal vessel density and choriocapillary flow deficit measurements. However, the measurements did differ between the two modes, highlighting the importance of selecting a consistent mode for longitudinal studies.

Acknowledgments

Disclosure: **F. Corvi**, None; **G. Corradetti**, None; **S. Parrulli**, None; **L. Pace**, None. **G. Staurenghi**, Heidelberg Engineering (C), Quantel Medical (C), Centervue (C), Carl Zeiss Meditec (C), Alcon (C), Allergan (C), Bayer (C), Boheringer (C), Genentech (C), GSK (C), Novartis (C), and Roche (C), Optos (F), Optovue (F), and Centervue (F). **S.R. Sadda**, Allergan (C), Amgen (C), Centervue (C), Genentech/Roche (C), Heidelberg (C), Novartis (C), Oxurion (C), and Optos (C); Carl Zeiss Meditec (I), Centervue (I), Nidek (I), Optos (I), and Topcon (I)

References

1. Spaide RF, Klancnik JMJ, Cooney MJ. Retinal vascular layers imaged by fluorescein angiography and optical coherence tomography angiography. *JAMA Ophthalmol.* 2015;133:45–50.
2. Spaide RF, Fujimoto JG, Waheed NK, Sadda SR, Staurenghi G. Optical coherence tomography angiography. *Prog Retin Eye Res.* 2018;64:1–55.
3. Spaide RF, Fujimoto JG, Waheed NK. Image artifacts in optical coherence tomography angiography. *Retina.* 2015;35:2163–2180.
4. Sadda SR. Defining the role of OCT angiography in clinical practice. *Ophthalmol Retin.* 2017;1:261–262.
5. Kashani AH, Chen C-L, Gahm JK, et al. Optical coherence tomography angiography: a comprehensive review of current methods and clinical applications. *Prog Retin Eye Res.* 2017;60:66–100.
6. Rocholz R, Corvi F, Weichsel J, Schmidt S, Staurenghi G, Bille JF, eds. OCT angiography (OCTA) in retinal diagnostics. In: *High Resolution Imaging*

- g in Microscopy and Ophthalmology: New Frontiers in Biomedical Optics* [Internet]. Ch. 6. Cham, Switzerland: Springer; 2019:135–160.
7. Magrath GN, Say EAT, Sioufi K, Ferenczy S, Samara WA, Shields CL. Variability in foveal avascular zone and capillary density using optical coherence tomography angiography machines in healthy eyes. *Retina*. 2017;37(11):2102–2111.
 8. Corvi F, Pellegrini M, Erba S, Cozzi M, Staurengi G, Giani A. Reproducibility of vessel density, fractal dimension, and foveal avascular zone using 7 different optical coherence tomography angiography devices. *Am J Ophthalmol*. 2018;18:25–31.
 9. Lei J, Pei C, Wen C, Abdelfattah NS. Repeatability and reproducibility of quantification of superficial peri-papillary capillaries by four different optical coherence tomography angiography devices. *Sci Rep*. 2018;8:17866.
 10. Corvi F, Cozzi M, Barbolini E, et al. Comparison between several optical coherence tomography angiography devices and indocyanine green angiography of choroidal neovascularization. *Retina*. 2020;40(5):873–880.
 11. Mihailovic N, Brand C, Lahme L, et al. Repeatability, reproducibility and agreement of foveal avascular zone measurements using three different optical coherence tomography angiography devices. *PLoS One*. 2018;13:e0206045.
 12. Parrulli S, Corvi F, Cozzi M, Monteduro D, Zicarelli F, Staurengi G. Microaneurysms visualisation using five different optical coherence tomography angiography devices compared to fluorescein angiography. *Br J Ophthalmol*, <https://doi.org/10.1136/bjophthalmol-2020-316817>. Online ahead of print.
 13. Borrelli E, Uji A, Sarraf D, Sadda SR. Alterations in the choriocapillaris in intermediate age-related macular degeneration. *Invest Ophthalmol Vis Sci*. 2017;58:4792–4798.
 14. Su L, Ji Y-S, Tong N, et al. Quantitative assessment of the retinal microvasculature and choriocapillaris in myopic patients using swept-source optical coherence tomography angiography. *Graefes Arch Clin Exp Ophthalmol*. 2020;258:1173–1180.
 15. Uji A, Balasubramanian S, Lei J, Baghdasaryan E, Al-Sheikh M, Sadda SR. Impact of multiple en face image averaging on quantitative assessment from optical coherence tomography angiography images. *Ophthalmology*. 2017;124:944–952.
 16. Kim AY, Chu Z, Shahidzadeh A, Wang RK, Puliafito CA, Kashani AH. Quantifying microvascular density and morphology in diabetic retinopathy using spectral-domain optical coherence tomography angiography. *Invest Ophthalmol Vis Sci*. 2016;57:OCT362–OCT370.
 17. Uji A, Balasubramanian S, Lei J, Baghdasaryan E, Al-Sheikh M, Sadda SR. Choriocapillaris imaging using multiple en face optical coherence tomography angiography image averaging. *JAMA Ophthalmol*. 2017;135:1197–1204.
 18. Spaide RF. Choriocapillaris flow features follow a power law distribution: implications for characterization and mechanisms of disease progression. *Am J Ophthalmol*. 2016;170:58–67.
 19. Zhang Q, Shi Y, Zhou H, et al. Accurate estimation of choriocapillaris flow deficits beyond normal intercapillary spacing with swept source OCT angiography. *Quant Imaging Med Surg*. 2018;8:658–666.
 20. Lei J, Durbin MK, Shi Y, et al. Repeatability and reproducibility of superficial macular retinal vessel density measurements using optical coherence tomography angiography en face images. *JAMA Ophthalmol*. 2017;135:1092–1098.
 21. Lee M-W, Kim K-M, Lim H-B, Jo Y-J, Kim J-Y. Repeatability of vessel density measurements using optical coherence tomography angiography in retinal diseases. *Br J Ophthalmol*, <https://doi.org/10.1136/bjophthalmol-2018-312516>. Online ahead of print.
 22. Al-Sheikh M, Tepelus TC, Nazikyan T, Sadda SR. Repeatability of automated vessel density measurements using optical coherence tomography angiography. *Br J Ophthalmol*. 2017;101:449–452.
 23. Ho J, Dans K, You Q, Nudleman ED, Freeman WR. Comparison of 3 mm × 3 mm versus 6 mm × 6 mm optical coherence tomography angiography scan sizes in the evaluation of non-proliferative diabetic retinopathy. *Retina*. 2019;39:259–264.
 24. Venugopal JP, Rao HL, Weinreb RN, et al. Repeatability of vessel density measurements of optical coherence tomography angiography in normal and glaucoma eyes. *Br J Ophthalmol*. 2018;102:352–357.
 25. Kurokawa K, Liu Z, Miller DT. Adaptive optics optical coherence tomography angiography for morphometric analysis of choriocapillaris [Invited]. *Biomed Opt Express*. 2017;8:1803–1822.
 26. Freund KB, Gattoussi S, Leong BCS. Dense B-scan optical coherence tomography angiography. *Am J Ophthalmol*. 2018;190:78–88.